have been obtained from anything but a differential reactor operated at steady state, and the present study emphasizes the usefulness of the recirculation type of differential reactor for studies of this type. Even though the kinetics are relatively complex, the stable activity of the sulfided cobalt molybdate catalyst and the fact that the stoichiometry follows a simple series type of reaction sequence without side products suggest that this may be also a useful model reaction.

ACKNOWLEDGMENT

The machine computations necessary in the preparation of this paper were performed at the Massachusetts Institute of Technology Computation Center. Acknowledgement is also made to the National Science Foundation for providing financial support to George W. Roberts in the form of a fellowship during the period of the project.

NOTATION

A = pre-exponential factor in Arrhenius expression for k or K
E = apparent activation energy in Arrhenius expression for k, kcal./mole
E_i = apparent heat of chemisorption of species i
f = fraction of butene molecules which hydrogenate at the original desulfurization site without first desorbing
$g(p_B)$ = function of butene partial pressure, g.-moles/(min.)(g. catalyst)
k = reaction rate constant, g.-moles/[(g. catalyst)(min.)(mm. Hg)]$^{(n_T+n_H)}$
K_i = adsorption constant of species i in Langmuir-Hinshelwood rate equations, mm. Hg^{-1}
n_D = power of denominator in Langmuir-Hinshelwood rate equations
n_i = reaction order with respect to species i in numerator of Langmuir-Hinshelwood rate equations
p_i = partial pressure of component i, mm. Hg
r_i = rate of disappearance or formation of species i, g.-moles/(g. catalyst)(min.)
R = gas constant, cal./(mole)(°K.)
T = absolute temperature, °K.

Subscripts

B = total butenes
C = butane
H = hydrogen
T = thiophene
S = hydrogen sulfide

Superscripts

′ = parameters used in rate equation for butane formation
″ = values of parameters if term $K_H p_H$ were introduced into Equation (4)

LITERATURE CITED

1. Griffith, R. H., J. D. F. Marsh, and W. B. S. Newling, *Proc. Roy. Soc. (London)*, **A197**, 194 (1949).
2. Kolboe, S., and C. H. Amberg, *Can J. Chem.*, **44**, 2623 (1966).
3. Komarewsky, V. I., and E. A. Knaggs, *Ind. Eng. Chem.*, **43**, 144 (1951).
4. Owens, P. J. and C. H. Amberg, *Advan. Chem. Ser.*, No. 33, 182 (1961).
5. Owens, P. J., and C. H. Amberg, *Can. J. Chem.*, **40**, 941 (1962).
6. Pease, R. N., and W. B. Keighton, Jr., *Ind. Eng. Chem.*, **25**, 1012 (1933).
7. van Looy, M., and G. Limido, *Compt. Rend. Congr. Intern. Chim. Ind.*, 31e, Leige (1958); *Ind. Chim. Belge.*, Suppl. 1, 645 (1959).
8. Roberts, G. W., Sc. D. thesis, Massachusetts Inst. Technol., Cambridge (1965).
9. ———, and C. N. Satterfield, *Ind. Eng. Chem. Fundamentals*, **5**, 317 (1966).
10. Kittrell, J. R., C. C. Watson, and W. G. Hunter, *AIChE J.*, **11**, 1051 (1965).
11. Kittrell, J. R., Reiji Mezaki, and C. C Watson, *Ind. Eng. Chem.*, **58**, No 5, 48 (1966).
12. Lapidus, Leon, and T. I. Peterson, *AIChE J.*, **11**, 891 (1965).

Manuscript received September 21, 1966; revision received May 15, 1967; paper accepted May 19, 1967.

Turbulent Flow in Concentric Annuli

CURTIS W. CLUMP

Lehigh University, Bethlehem, Pennsylvania

DANIEL KWASNOSKI

Bethlehem Steel Corporation, Bethlehem, Pennsylvania

An eddy diffusivity model was developed and used to predict velocity distributions for turbulent flow of air in annuli. Comparison of distributions calculated by the model with experimental data shows that good agreement between calculated and measured values can be attained for core-to-shell ratios from 0.001 to 0.990. The significant advantage of using a diffusivity model to predict velocity distributions lies in the inherent ability to consider systems with nonlinear stress distributions.

Fully developed turbulent flow of a Newtonian fluid in smooth concentric annuli is of interest to the engineer because of its direct engineering applications and to the scientist because it can provide insight into the problem of developing a complete theory of turbulent flow. The two limiting cases of one-dimensional fully developed turbulent flow in annuli have been studied in detail. They are flow in circular pipes and flow between parallel flat plates. For flows of these types the velocity distributions can be predicted within the accuracy of experimental data with the use of various universal velocity distribution laws (*2, 5, 9, 11*). Although better predictions would be ob-

tained if the laws were modified to include the effect of Reynolds number, their utility is evident from their widespread engineering applications.

For flow in annuli the predictions obtained from the universal velocity distribution laws are in obvious disagreement with experimental data (*1, 4*). This discrepancy arises for two reasons. First, fully developed annular flow exists within two regions, each extending from a wall to a point of maximum velocity. Unlike the case of flow through pipes and flow between parallel flat plates where the point of maximum velocity is midway between opposing walls, for annular flow the point of maximum velocity lies nearer the core wall. Second, the shear stress is not a linear function of distance from the wall, particularly for annuli with small core-to-shell ratios. For flow through pipes and flow between parallel flat plates, the shear stress distributions are essentially linear.

Sparrow et al. (*10*) acknowledged the presence of a nonlinear stress distribution in a study of flow longitudinal to a cylinder. They applied a stress distribution of the form

$$\frac{\tau}{\tau_w} = \frac{r}{r+x} \tag{1}$$

to the shear stress-eddy diffusivity relationship

$$\frac{\tau}{\tau_w} = \left(1 + \frac{\epsilon}{\nu}\right)\frac{du^+}{dy^+} \tag{2}$$

and determined universal velocity distributions by numerically integrating Equation (2).

This method can be extended to study flow in annuli in which the shear stress distributions can be rigorously calculated from simple force balances when the maximum velocity radius is known. The modified u^+ y^+ relationships obtained can then be compared with experimental data and universal velocity distribution predictions to determine the applicability of diffusivity models.

The exact location of the maximum velocity for turbulent annular flow, which is needed to calculate the shear stress distributions used in a diffusivity model, is under disagreement. Rothfus (*6*) and Knudsen and Katz (*4*) concluded that the location of the maximum velocity for turbulent flow was essentially the same as that for laminar flow. More recent work by Brighton and Jones (*1*) suggests that the location of the maximum velocity for turbulent flow in annuli is different from that of laminar flow, with the location being a function of the Reynolds number and the core-to-shell ratio of the annulus.

The relationship between eddy diffusivity and velocity gradient is also subject to disagreement. The purely phenomenological eddy diffusivity expressions of von Karman (*11*) and others (*3*) have been criticized because in many instances the assumed mechanics of turbulent transport have been experimentally proven to be incorrect. In spite of these shortcomings, the phenomenological models have not been replaced to any great extent by current efforts to describe the actual turbulent transport mechanism.

For this work, the eddy diffusivity-velocity gradient equations derived by Deissler (*2*) from von Karman's diffusivity expressions were employed. Because of the obvious disagreement in the location of the maximum velocity radius, the study was repeated for two cases: (1) The laminar and turbulent maximum velocity radii were assumed identical as proposed by Rothfus and Knudsen and Katz; and (2) an expression based on the experimental data of Brighton and Jones to locate the maximum velocity radius was employed.

ANALYSIS OF ANNULAR FLOW

The stress distribution functions for flow in an annulus can be obtained from simple force balances. These balances are written across two flow regions, one bounded by the shell and the maximum velocity radius and the other by the maximum velocity radius and the core. The resulting normalized shear stress distribution for the region bounded by the maximum velocity radius and the shell wall of the annulus is

$$\frac{\tau}{\tau_2} = \left[\frac{r_m^2 r_2}{r_m^2 - r_2^2}\right]\left[\frac{1}{r} - \frac{r}{r_m^2}\right]; \quad r_2 > r > r_m \tag{3a}$$

Similarly, for the region bounded by the maximum velocity radius and the core wall of the annulus, the normalized shear stress distribution is given by

$$\frac{\tau}{\tau_1} = \left[\frac{r_m^2 r_1}{r_m^2 - r_1^2}\right]\left[\frac{1}{r} - \frac{r}{r_m^2}\right]; \quad r_m > r > r_1 \tag{3b}$$

Equations (3*a*) and (3*b*) can be used to calculate the shear stress distribution for any annulus when the maximum velocity radius is known. Two methods of determining the maximum velocity radius that represent the extremes of published experimental data were employed in this work. The first is based on the assumption that the radius of maximum velocity is identical for both laminar and turbulent flow and is given by

$$r_m = r_2\left[\frac{1-(r_1/r_2)^2}{2\ln(r_2/r_1)}\right]^{0.5} \tag{4}$$

The second method for determining the location of the maximum velocity is based on equations obtained from standard polynomial curve-fitting techniques (*8*) applied to the data of Brighton and Jones. Although the data indicate a slight Reynolds number effect at small core-to-shell ratios, it was excluded from this work. The expressions obtained relate the maximum velocity to core-to-shell ratio as follows:

$$r_m = r_1 + \left[\left[\frac{r_2 - r_1}{2}\right]\left[1.08\left(\frac{r_1}{r_2}\right)^3 - 2.20\left(\frac{r_1}{r_2}\right)^2 + 1.65\left(\frac{r_1}{r_2}\right) + 0.48\right]\right] \tag{5}$$

for core-to-shell ratios between 0.0625 and 1, and

$$r_m = r_1 + [18.1\,(r_2 - r_1)]\frac{r_1}{r_2} \tag{6}$$

for core-to-shell ratios less than 0.0625.

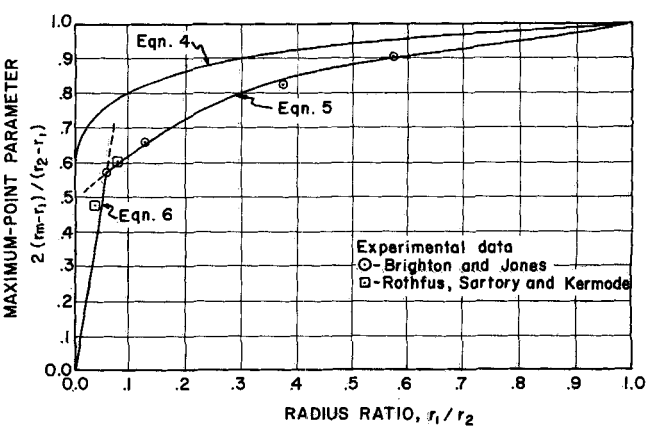

Fig. 1. Position of maximum point in annuli at high Reynolds numbers (solid line indicates predicted values).

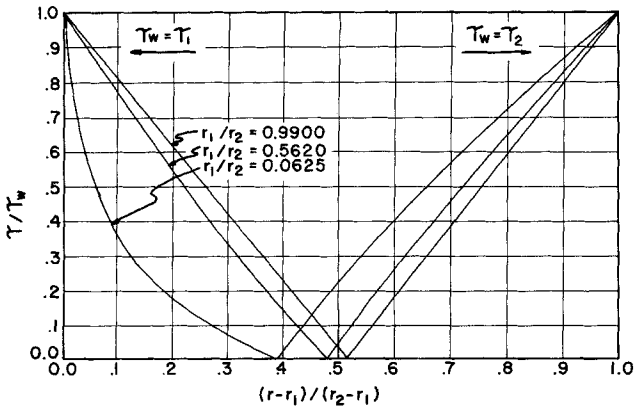

Fig. 2. Normalized shear stress distributions [r_m calculated from Equation (4)].

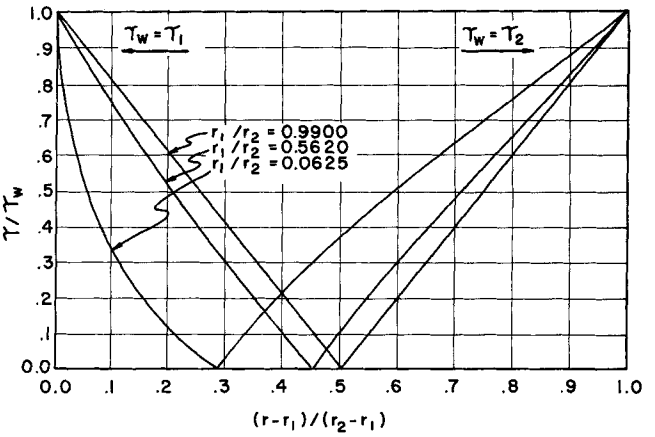

Fig. 3. Normalized shear stress distributions [r_m calculated from Equations (5) and (6).]

A comparison of the maximum velocity location calculated with Equation (4) and Equations (5) and (6) over a broad range of annuli core-to-shell ratios is presented in Figure 1. Figure 2 shows the effect of core-to-shell ratio on shear stress distribution for concentric annuli when Equations (3*a*), (3*b*), and (4) are used. Figure 3 shows the effect when Equations (5)and (6) are combined with Equations (3*a*) and (3*b*).

Employing the definition of eddy diffusivity, one can write a simple stress equation as

$$\tau_{gc} = (\mu + \rho\epsilon)\frac{du}{dy} \tag{7}$$

Combination of Equation (7) with Equations (3*a*) and (3*b*) gives the following expressions describing the velocity distributions for the outer and inner regions of flow:

$$\frac{du_2}{dy_2} = \left[\frac{\tau_2 g_c}{\mu + \rho\epsilon}\right]\left[\frac{r_m^2 r_2}{r_m^2 - r_2^2}\left[\frac{1}{r} - \frac{r}{r_m^2}\right]\right] \tag{8a}$$

$$\frac{du_1}{dy_1} = \left[\frac{\tau_1 g_c}{\mu + \rho\epsilon}\right]\left[\frac{r_m^2 r_1}{r_m^2 - r_1^2}\left[\frac{1}{r} - \frac{r}{r_m^2}\right]\right] \tag{8b}$$

Equations (8*a*) and (8*b*) can be converted to

$$\frac{du_2^+}{dy_2^+} = \left[\frac{r_m^2 r_2}{(r_m^2 - r_2^2)\left(1 + \frac{\epsilon}{\nu}\right)}\right]\left[\left[\frac{u_2^*}{u_2^* r_2 - y_2^+ \nu}\right] - \left[\frac{u_2^* r_2 - y_2^+}{u_2^* r_m^2}\right]\right] \tag{9a}$$

$$\frac{du_1^+}{dy_1^+} = \left[\frac{r_m^2 r_1}{(r_m^2 - r_1^2)\left(1 + \frac{\epsilon}{\nu}\right)}\right]\left[\left[\frac{u_1^*}{u_1^* r_1 + y_1^+ \nu}\right] - \left[\frac{u_1^* r_1 - y_1^+}{u_1^* r_m^2}\right]\right] \tag{9b}$$

To solve these expressions a relationship among eddy diffusivity, velocity, and velocity gradient is required. Deissler (2) derived two convenient expressions from von Karman's diffusivity expressions:

$$\frac{\epsilon}{\nu} = n^2 u^+ y^+; \quad y^+ < 26 \tag{10}$$

$$\frac{\epsilon}{\nu} = K^2\left(\frac{du^+}{dy^+}\right)^3 \Big/ \left(\frac{d^2u^+}{dy^{+2}}\right)^2; \quad y^+ > 26 \tag{11}$$

By employing Equations (10) and (11), one can integrate Equations (9*a*) and (9*b*) to obtain the universal velocity distributions for the two regions of flow.

DEVELOPMENT OF A DIFFUSIVITY MODEL

The model discussed here is essentially a systematic method of solving the differential universal velocity distribution Equations (9*a*) and (9*b*). Numerical techniques are available to integrate equations of these types (8), but the limits of integration must first be established. When Equation (10) is used no problem exists because the limits are set, by definition, at $y^+ = 0$ and $y^+ = 26$. For Equation (11), however, the expressions (9*a*) and (9*b*) must be integrated from $y^+ = 26$ to some as yet undetermined value of y^+ where the velocity is a maximum. This problem can be resolved by observing that at $y^+ = y^+_m$, the following relationship must also be satisfied:

$$u^+_m = \frac{u_m y_m}{y^+_m \nu} \tag{12}$$

A trial and error approach can then be used to solve the differential equations. In this work, the following procedure was used:

1. Assume a value for u^+_m
2. Calculate u^* from the expression

$$u^* = \frac{u_m}{u^+_m} \tag{13}$$

3. Calculate y^+_m from the relationship

$$y^+_m = \frac{u^* y_m}{\nu} \tag{14}$$

4. Integrate Equation (9*a*) from $y^+ = 0$ to $y^+ = 26$ using Equation (10) and a numerical method for solving equations of the first order.
5. Integrate Equation (9*a*) from $y^+ = 26$ to $y^+ = y^+_m$ using Equation (11) and a numerical method for solving equations of the second order.
6. Compare the value of u^+_m obtained from the integration with the assumed value of step 1.
7. Modify the assumed value of u^+_m and repeat steps 1 through 6 until the desired agreement is reached between the assumed and calculated values of u^+_m.
8. Repeat steps 1 through 7 for the integration of Equation (9*b*).

To facilitate the calculations this trial and error pro-

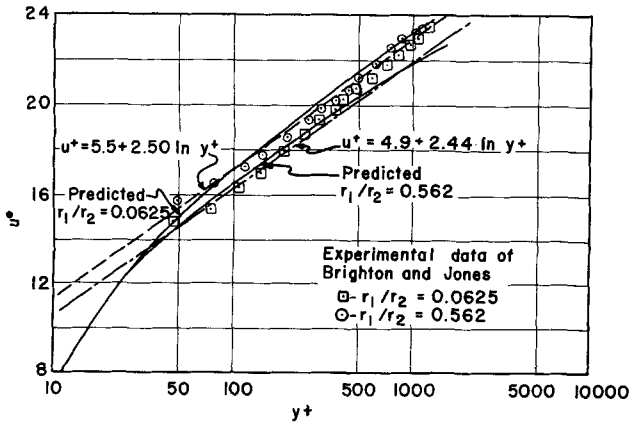

Fig. 4. Comparison of predicted and experimental velocity distributions for the law of the wall (outer profile) at a maximum velocity of 60 ft./sec.

cedure was programmed for the IBM 1620 digital computer. The differential equations coupled with Equation (10) were solved with the use of the modified Euler method, because derivatives of the first order only are involved. To start this method the initial conditions of $u^+ = 0$ and $du^+/dy^+ = 1$ at $y^+ = 0$ are used. The integration then proceeds in y^+ increments calculating and correcting u^+ for each forward step. Only two points are needed for each calculation, the previous point and the new point. The value of u^+ at the new point is first calculated using the slope at the old point and an increment distance in the y^+ direction. For each point the procedure was repeated until the change in u^+ for the new point was less than 0.001. It was found that tests with increments from 0.1 to 0.5 produced essentially no change in the u^+ y^+ distribution and a value of 0.5 was deemed satisfactory for subsequent integrations.

To integrate the differential expressions coupled with Equation (11), the second-order Runge-Kutta method was used. This method is not iterative. A single solution is obtained by applying the set of formulas of Runge and Kutta (8). Tests of this method with increment sizes from 0.1 to 0.5 again showed essentially no change in the u^+ y^+ distributions obtained and a value of 0.5 was selected for the balance of the integrations.

Because the shear stresses at the walls of the annulus are calculated with a model of this type, universal velocity distributions are readily converted to mean velocity profiles. Additional information, such as velocity gradients and average velocities, can also be computed with a slight increase in machine time.

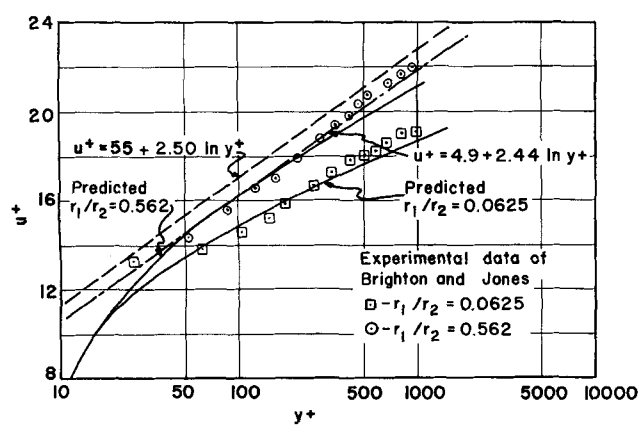

Fig. 5. Comparison of predicted and experimental velocity distributions for the law of the wall (inner profile) at a maximum velocity of 60 ft./sec.

TESTING THE MODEL

The model was tested for annuli with 8-in. shells and 0.5- and 4.5-in. cores, or core-to-shell ratios of 0.0625 and 0.562, respectively. Calculations were performed for air flowing at maximum velocities of 30 and 60 ft./sec. These conditions were employed by Brighton and Jones (1) in their experimental work, and their application afforded a direct comparison between calculated and experimental results.

Throughout the tests the coefficients n and K in Equations (10) and (11) were varied until the best fit between calculated and experimental results was obtained. The following relationships were found to give the most acceptable values for the coefficients:

$$n = 0.109 + (0.00038y^+)\,\alpha \qquad (15)$$

$$K = 0.360 + \left(\frac{4.0}{y^+}\right)\alpha \qquad (16)$$

In these equations α has the value $(r_m - r_1)/(r_2 - r_m)$ when calculating velocity distributions for the outer region and $(r_2 - r_m)/(r_m - r_1)$ when distributions are calculated for the inner region of flow. In Figures 4 and 5 the universal velocity distributions predicted by the model are compared with the experimental data of Brighton and Jones and with velocity distributions predicted by two of the published universal velocity distribution laws. As shown in these figures, the distributions obtained from the model are in good agreement with the experimental data. Unlike the published universal velocity distribution laws that predict the same distribution for the inner and outer regions of flow, the model predictions show the marked difference between the distributions for the two regions.

The universal velocity distributions were then converted to their corresponding mean velocity profiles for further comparison with experimental data. This was done by employing the definitions of u^+ and y^+ at their maximum values to evaluate the shear stresses at the shell and core walls. Direct relationships are obtained between the mean and universal velocities. Figure 6 shows a comparison of the experimental data of Brighton and Jones with the

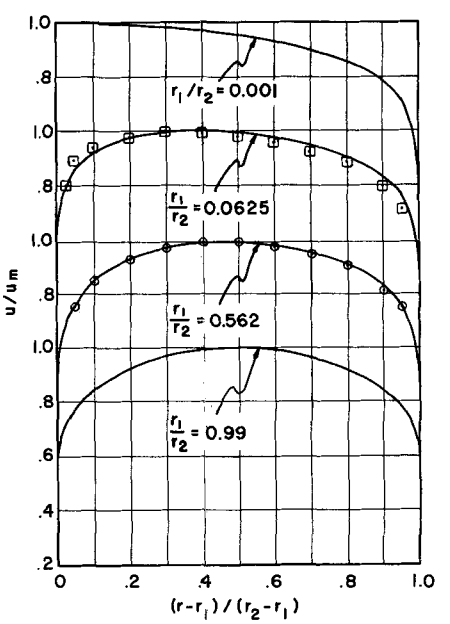

Fig. 6. Comparison of predicted velocities with the experimental data of Brighton and Jones at a maximum velocity of 60 ft./sec. (solid line indicates predicted profile).

mean velocity profiles obtained from the universal velocity distributions of Figures 4 and 5.

A final test of the model was made at the extreme conditions of an annulus having a very small core-to-shell ratio (approaching tube flow) and a very large core-to-shell ratio (approaching flow between parallel flat plates). Core-to-shell ratios of 0.001 and 0.990 and a maximum velocity of 60 ft./sec. were employed. Results obtained for the mean velocity profiles are shown in Figure 6. As the figure depicts, the model produces the velocity distributions expected at these conditions.

DISCUSSION

To employ the diffusivity concept to a given system, the nonlinear stress distributions must either be known or readily calculable. For the case of annular flow considered in this work, simple force balances were employed to calculate the distributions. A shortcoming in the theory of turbulent flow made it necessary to rely on assumptions or experimental data to determine the location of the maximum velocity on which the results of the force balances rely.

The best fit between distributions calculated by the model and the experimental data of Brighton and Jones was obtained when Equations (5) and (6) were used to locate the point of maximum velocity. Although it could be argued that the model predictions fit the data simply because the data were used in its development, a comparison of the predicted universal velocity distributions with the published experimental data of Knudsen and Katz (*4*) shows that good agreement is also obtained.

Because the mean velocity profile is somewhat flat at the point of maximum velocity, it is difficult to measure this point experimentally. The model, however, calculates this point directly and substantiates the data of Brighton and Jones that show the location of the maximum velocity for turbulent flow in annuli to be quite different from that for laminar flow. This statement is made because the model uses the point of maximum velocity to calculate both the universal and the mean velocity distributions; and the predicted universal velocity distributions are in good agreement with the published data of other investigators (*4*). Good agreement between the model predictions and the published data could not be found when Equation (4) was used to locate the point of maximum velocity.

Velocity distributions for turbulent annular flow can be predicted from the proposed model with a minimum of information. The needed data are core radius of annulus (ft.), shell radius of annulus (ft.), an average or maximum velocity flow (ft./sec.), kinematic viscosity of the fluid (sq.ft./sec.).

If an average velocity is used an iterative procedure is required for solution. The time required to calculate a profile varies with the number of iterations performed. For the results shown here the average running time on an IBM 1620 computer was about 15 min.

A recent paper (*7*) gives results which are in excellent agreement with the predicted values presented here. The authors propose a method for predicting velocity profiles in smooth concentric annuli at high Reynolds numbers from the profiles in equivalent tubes. To meet the imposed constraints, it was necessary to imagine that the inner part of the annulus carried a fluid with neither the density nor the viscosity of the actual one. It was interesting to note that in the method presented here the same conditions are observed and inherently considered by the parameters n and K defined by Equations (15) and (16).

In their recent publication, Rothfus et al. (*7*) employed the following equation to relate radius of maximum velocity to radius ratio for highly turbulent flow in annuli:

$$2\frac{(r_m - r_1)}{(r_2 - r_1)} = (r_1/r_2)^{0.2}$$

This equation fits the data of Brighton and Jones very well for annuli with radius ratios to 0.0625. From their experimental work, Rothfus et al. showed that its application can be extended to radius ratios as low as 0.026. The more complicated equations, (5) and (6), used in the present work can then be replaced by this one simple equation.

NOTATION

g_c = conversion factor, 32.2 (lb.$_m$) (ft.)/(lb.$_f$) (sec.^{2})
K = parameter as defined by Equation (11), dimensionless
L = length of ducts, ft.
n = parameter as defined by Equation (10), dimensionless
r = radial distance, ft.
r_m = radius of maximum velocity, ft.
u = time-average local axial velocity, ft./sec.
u_m = maximum time-average axial velocity, ft./sec.
u^+ = universal velocity, u/u^*, dimensionless
u^+_m = maximum universal velocity, dimensionless
u^* = friction velocity, $\sqrt{\tau_w g_c/\rho}$, ft./sec.
x = constant in Equation (1), dimensionless
y = distance from tube wall, ft.
y^+ = universal distance, $y\sqrt{\tau_w g_c/\rho}/\nu$, dimensionless
y^+_m = maximum universal distance, dimensionless

Greek Letters

α = coefficient in Equations (15) and (16)
ϵ = eddy diffusivity of momentum, sq.ft./sec.
ν = molecular diffusivity of momentum, μ/ρ, sq.ft./sec.
μ = viscosity of fluid, lb.$_m$/(ft.) (sec.)
ρ = density of fluid, lb.$_m$/cu.ft.
τ = shearing stress, lb.$_f$/sq.ft.
τ_w = shearing stress at the tube walls, lb.$_f$/sq.ft.

Subscripts

m = position of zero shear or maximum time-average local velocity
w = wall of the annulus
1 = inner surface of the annulus or the portion inside the maximum point
2 = outer surface of the annulus or the portion outside the maximum point

LITERATURE CITED

1. Brighton, J. A., and J. B. Jones, *J. Basic Eng.*, 835-844 (1964).
2. Deissler, R. G., *Natl. Advisory Committee Aeronaut. Tech. Note TN 3145* (1954).
3. Hinze, J. O., "Turbulence," McGraw-Hill, New York (1959).
4. Knudsen, J. G., and D. L. Katz, *Midwestern Conf. Fluid Dynamics*, 175-203 (1950).
5. Rannie, W. D., *J. Aeron. Sci.*, **23**, 485-489 (1956).
6. Rothfus, R. R., Ph.D. thesis, Carnegie Inst. Technol. Pittsburgh, Pa. (1948).
7. ———, W. K. Sartory, and R. I. Kermode, *AIChE J.*, **12**, 1086-1091 (1966).
8. Scarborough, J. B., "Numerical Mathematical Analysis," 5 ed., Johns Hopkins Press, Baltimore (1962).
9. Spalding, D. B., *J. Appl. Mech.*, **28**, 455-457 (1961).
10. Sparrow, E. H., E. R. G. Eckert, and W. J. Minkowycz, *ibid.*, **42**, 37 (1963).
11. von Karman, Th., *Trans. Am. Soc. Mech. Eng.*, **61**, 705-710 (1939).

Manuscript received March 10, 1967; revision received May 29, 1967; paper accepted May 31, 1967.